IEICE Proceeding Series

Complex Network Analysis of Retinotopic Maps in the Human Brain

Tetsuya Shimokawa, Kenji Leibnitz, Ferdinand Peper

Vol. 2 pp. 122-125
Publication Date: 2014/03/18
Online ISSN: 2188-5079

2013 International Symposium on Nonlinear Theory and its Applications
NOLTA2013, Santa Fe, USA, September 8-11, 2013

Complex Network Analysis of Retinotopic Maps in the Human Brain

Tetsuya Shimokawa†, Kenji Leibnitz†, and Ferdinand Peper†

†Center for Information and Neural Networks (CiNet), National Institute of Information and Communications Technology, and Osaka University, 1-4 Yamadaoka, Suita, Osaka 565-0871, Japan
Email: shimokawa@nict.go.jp

Abstract—The use of complex network analysis to brain imaging has been instrumental to a deeper understanding of the way the brain works at a system level. The more traditional method embodied by Statistical Parametric Mapping (SPM) is limited to the testing of hypotheses through statistical processes about specific effects in localized *Regions of Interest*. In order to check the validity of complex network analysis from the viewpoint of SPM, we analyze fMRI data for retinotopic maps, utilizing established knowledge concerning SPM.

1. Introduction

Human brain mapping in the 1980's was mainly aimed at characterizing how specialized *regions of interest* (ROI; e.g., [1]) in the brain respond to differences in experimental conditions. Though this reduces the huge number of voxels to a tractable ROI measurement, it fails to map new functional brain regions (whole-brain analysis). The study of more global effects involving many ROIs requires the use of statistical maps. Statistical parametric mapping (SPM) is one of the most well-established statistical techniques for the analysis of brain imaging data (fMRI, MEG, PET, etc.) [2, 3]. Widely used in brain research, SPM entails the construction of statistical processes to test hypotheses about regionally specific effects. In recent years brain research has seen an increasing interest in complex network analysis [4]—a multidisciplinary approach in which the properties of complex systems are described by quantifying network topologies based on graph theory. Unlike SPM, which extracts specific brain regions associated with a statistically-significant increase of the response to a stimulus, complex network analysis uncovers the specific link topologies between brain regions that have significant correlations in response to stimuli.

An important measure of the structure of a network is *modularity*, which is the extent to which a network can be divided into clusters of nodes that have higher densities of connections between intra-cluster nodes than inter-cluster nodes [5]. Modules in networks can be determined using heuristic algorithms, like the *Louvain method* [6], in a time that is only a logarithmic factor larger than the number of nodes. Identification of modules in brain networks is important, because they tend to correspond with functional units in the brain. Modularity on not only one topological scale, but also on various scales has attracted attention in brain research, because it is thought to enhance reconfigurability of connections without affecting stability of network dynamics [5].

Ideally, if SPM analysis would be applied to the extraction of networks in the brain, the validity of complex network analysis in brain research could be evaluated, but unfortunately the significant corpus of results from SPM analysis has remained out of reach due to the incompatibility of both analysis methods.

This paper investigates how both methods can be compared by restricting ourselves to a so-called *retinotopical* experiment. Retinotopy is the mapping of a visual stimulus on the retina to an area of the visual cortex. In this report, we analyze the fMRI data for retinotopic maps for three different simple visual stimuli, and make a comparison with corresponding SPM results, of which we have an extensive analysis available. Our results show a clear performance difference in network analysis between the whole-brain on one hand and the early stages of the visual cortex only on the other hand. If we restrict ourselves to the above visual areas, we are able to identify three different modular sub-networks corresponding to the three stimuli, but this becomes impossible for whole-brain networks. When hierarchical modularity is assumed in our analysis, however, we can extract some of the modules for specific visual stimuli, even if we deal with whole-brain networks. Overall, the properties we find in the analysis of networks are compatible with SPM results, but the extracted modules are usually the mixture of two stimuli. We discuss the reason for the occurrence of these mixtures, and conclude that the results between the different methods resemble each other sufficiently close to validate network analysis methods in brain imaging research.

2. Methods

The visual stimuli used in the experiment consist of three sizes of rings, denoted by *center* (Fig. 1(a)), *middle* (Fig. 1(b)), and *peripheral* (Fig. 1(c)) in order of increasing radii. Each ring is composed of a high-contrast checkerboard, the fields of which change synchronously in an ON-OFF fashion. The experiment is organized in three sessions, each consisting of six groups (Fig. 1(e)). In one group there are four epochs, the first three of which correspond to the respective stimuli, and the last one of which is a resting state (no stimuli; Fig. 1(d)). Inside each epoch

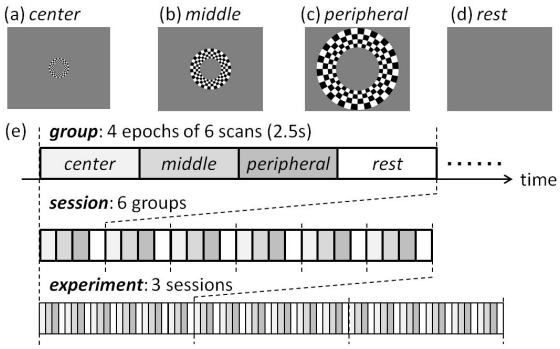

Figure 1: (a)-(d) Visual stimuli. (e) Organization of experiment.

six fMRI scans are made, each taking 2.5 s, so each epoch takes 15 s. During an epoch, the corresponding stimulus is shown to the subject.

3. Results

3.1. Activated Region (SPM-t Image)

In order to estimate the activated region for specific visual stimuli, we extract the fMRI data by using the *hrf* (haemodynamic response function) in Fig. 2(a). This is an impulse response function of the stimulus, represented by the response of blood oxygen levels. The output of the impulse response function is the convolution integral of the *hrf* and the function describing the actual stimulus. In Fig. 2(b), the function resulting from the convolution integral is superimposed on the time-series of the fMRI output signal. Suppose that the extracted functions for the *center*-, the *middle*-, and the *peripheral*-stimulus are $x_1(t)$, $x_2(t)$, and $x_3(t)$, respectively. Then the time-series of the fMRI data, $y(t)$, can be estimated as the linear sum of the three convolved functions $x_i(t)$ for $i = 1, 2, 3$ as

$$y(t) = \beta_0 + \beta_1 x_1(t) + \beta_2 x_2(t) + \beta_3 x_3(t) + error.$$

The result is called the General Linear Model (GLM). Statistically, we can estimate the three parameters β_i for $i = 1, 2, 3$ by minimizing the root-mean-square of the error term. When we want to identify the activated region for, for example the *center*-stimulus, we test the estimation of β_i under the null hypothesis $\sum_i c_i\beta_i = 0$, where c_i is the contrast vector chosen such that the sum of the three elements is zero, and only one element contributes in a positive way; here $\{c_1, c_2, c_3\} = \{1, -0.5, -0.5\}$ is used for the *center*-stimulus. In Fig. 2(b), the green graph is the original time-series, and the blue graph is $\sum_i \beta_i x_i(t)$ with the β_i as estimated above. Fig. 3.1 shows the activated brain region for the *center*-stimulus, which is displayed by the SPM toolbox in MATLAB. For the *middle*-stimulus we set $\{c_1, c_2, c_3\} = \{-0.5, 1, -0.5\}$ and for the *peripheral*-stimulus $\{c_1, c_2, c_3\} = \{-0.5, -0.5, 1\}$.

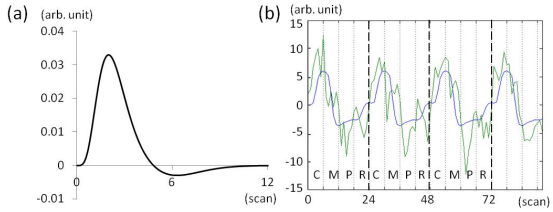

Figure 2: (a) Haemodynamic response function used in SPM. (b) Time series at the voxel (22,-106,8), which is the voxel with maximal response for the *center*-stimulus.

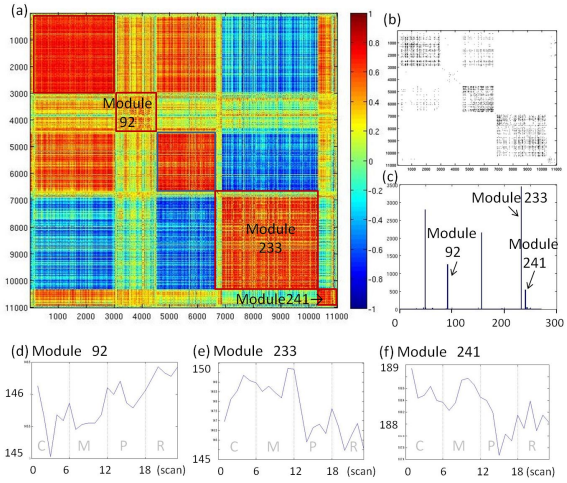

Figure 3: Network properties for the whole-brain network. (a) correlation matrix, (b) adjacency matrix (threshold is 0.8), (c) histogram of the number of elements in each module (abscissa is module number). (d)-(e) are the averaged time-series.

3.2. Whole Brain Network

Fig. 3(a) shows the correlation matrix for the whole-brain data when all visual stimuli are taken into account. This correlation matrix is arranged such that elements belonging to the same module lie near each other in a block with similar colors. The modules are estimated by the Louvain algorithm[6] and labeled as in Fig. 3.

As shown in the histogram in Fig. 3(c), there are five dominant modules. Fig. 3(d)-(f) shows the averaged time-series for three of those modules, whereby the abscissa indicates the scan number. Suppose that the time-series at a voxel is described as the numerical sequence $\{y_1, y_2, \cdots\}$, so y_n is the value of the voxel in the n-th scan. The averaged time-series are defined as

$$\tilde{y}_k = \frac{1}{N}\sum_{n=0}^{N-1} y_{k+24n}, \qquad k = 1, 2, \cdots, 24,$$

where N is the total number of groups in one experiment ($N = 3$ sessions $\times 6$ groups $= 18$). The range of k for the *center*-, *middle*-, *peripheral*-, and *rest*-epoch corresponds

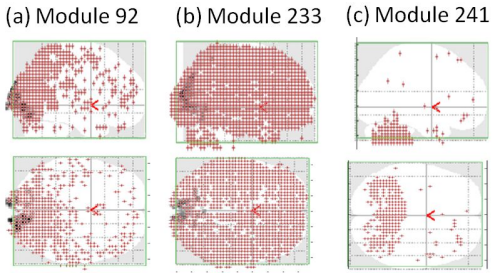

Figure 4: Comparison between activated region (SPM-t image) and estimated module region (by the Louvain method) for (a) module 92 (with black SPM for *middle*), (b) module 233 (with black SPM for *peripheral*), and (c) module 241 (without black SPM).

to $k \in [1, 6]$, $k \in [7, 12]$, $k \in [13, 18]$ and $k \in [19, 24]$, respectivelly.

Figure 4 shows the distribution of the voxels corresponding to each module in the brain. Voxels belonging to module 92 appear to be mainly distributed in the area of the visual cortex, whereas voxels in module 233 are uniformly distributed over the whole brain. Voxels in module 241 are mostly limited to locations in the cerebellum, which is related to motor control, and not to visual processing. The averaged time-series in Fig. 3(d)-(f) are dissimilar to the haemodynamic response function in Fig. 2(a), and neither do they show significant differences between the scans belonging to the different stimuli. One possible reason is that the connection among voxels in visual cortex is not strong enough to extract stimulus-related modules, because some of connections can be indirect correlation through the common stimulus pattern. We conclude that we cannot differentiate between any clustered sub-networks for different visual stimuli for the whole-brain data.

3.3. Truncated Network

In order to overcome the problem mentioned in the previous section, we truncate the brain network so that only the region predicted to be significant by SPM is included. As shown in Fig. 5 and Fig. 6, we can clearly find three different modular sub-networks for the three different visual stimuli. In Fig. 6, the plotted red points for each estimated module are almost superimposed on the values obtained from SPM (black map). The boundaries of the estimated modules are similar to the corresponding boundaries obtained from SPM. Fig. 5(f) is similar to the *hrf* for the *peripheral*-stimulus. Fig. 5(d) appears to be a mixture of both *center*- and *middle*-stimulus modules, and Fig. 5(e) appears to be a mixture of both *middle*- and *peripheral*-stimulus modules.

3.4. Hierarchical Modularity in Whole-Brain Network

Even if we deal with the whole-brain network, we can extract some of the modules for specific visual stimuli by

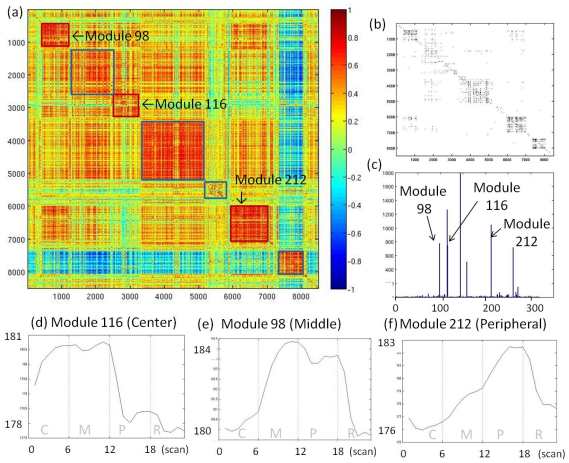

Figure 5: Network properties for the truncated brain network. (a) Correlation matrix, (b) Adjacency matrix (threshold is 0.8), (c) Histogram of the number of elements in each module (abscissa is module number). (d)-(e) are the averaged time-series.

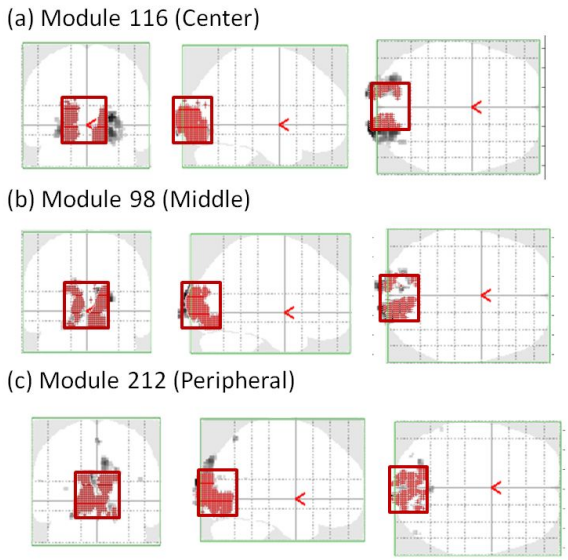

Figure 6: Comparison between activated region (SPM-t image, black) and estimated module region (red dot, estimated by the Louvain method) for (a) the *center*-stimulus (module 116), (b) the *middle*-stimulus (module 98), and (c) the *peripheral*-stimulus (module 212). Truncated boundaries are shown as red rectangles.

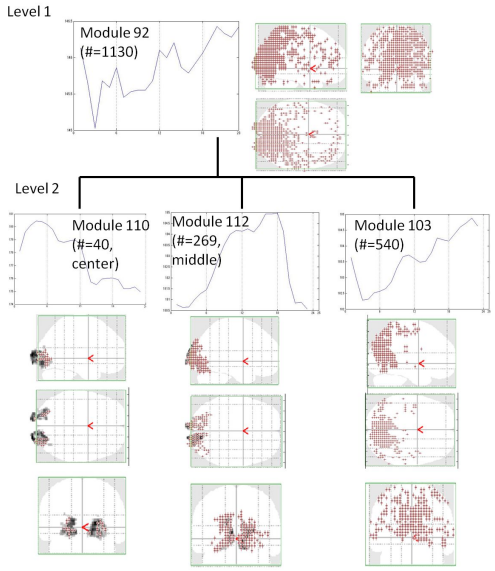

Figure 7: Hierarchical modularity, calculated by the Louvain method. Module 92 in level 1 is the same as module 92 in Fig. 4(a).

extracting hierarchical modularity (estimated by the Louvain method). Module 110 (level 2) in Fig. 7 appears to be a mixture of both *center*- and *middle*-stimuli. The black region is SPM-related for the *center*-stimulus. Red points related to module 110 (level 2) are located mostly within the black region related to SPM. Module 112 (level 2) in Fig. 7 appears to be a mixture of both *middle*- and *peripheral*-stimulus modules. The black region is SPM-related for the *middle*-stimulus. Red points related to module 112 (level 2) are partially located outside the black region belonging to SPM, but partially have the same boundaries.

4. Discussion

The complex networks obtained from fMRI data of the retinotopic experiment in this paper are compatible with the results from SPM. However, the extracted modules do not have a pure correspondence with the three checkerboard patterns stimuli, but rather tend to be based on a mixture of two out of the three stimuli. Among the five modules identified from whole-brain data, there are three modules for which the fMRI signal goes up and then down once in four epochs, whereas in the other two modules the signal does so twice in four epochs. The latter two modules are thus more dominant in terms of correlated activity, indicating increased connectivity between these modules, as compared with the first three modules (see also Fig. 8).

The major advantage of complex network-based analysis compared with SPM is that while SPM shows only the coordinates of voxels in the activated regions, modules estimated by complex network analysis show the connectivity among voxels as well as their coordinates. Traditionally, cytoarchitecturally labeled brain area (like, Brodmann area) is used as the candidate of ROIs. However, such anatomical difference does not always explain the functional difference in the brain activity. The modules estimated by complex network analysis can be a new candidate of ROIs which can clearly explain the functional difference in the whole-brain networks.

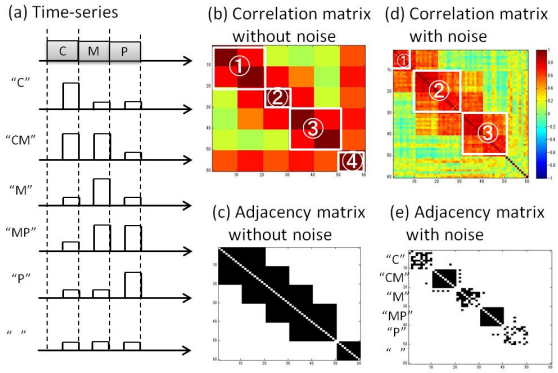

Figure 8: Simulated time-series, the correlation matrix, and the adjacency matrix. Estimated modularity by the Louvain algorithm are shown on the correlation matrix with white boxes. Noise is uniformly distributed from -0.4 to 0.4. One epoch stimulus include 10 points, and noise is i.i.d for all points. Threshold for the adjacency matrix is 0.7.

Acknowledgments

The authors appreciate the help from Yusuke Morito during experiments and processing the fMRI data.

References

[1] P.T. Fox, M.A. Mintun, M.E. Raichle, *et al.* "Mapping human visual cortex with positron emission tomography," *Nature*, vol. 323, pp. 806-809, 1986.

[2] Wellcome Trust Centre for Neuroimaging, "Statistical parametric mapping toolbox," available online at: http://www.fil.ion.ucl.ac.uk/spm/

[3] K. Friston, *et al.,* Statistical Parametric Mapping, Academic Press, 2007.

[4] O. Sporns, Networks of the Brain, MIT Press, 2011.

[5] D. Meunier, R. Lambiotte, E.T. Bullmore, "Modular and hierarchically modular organization of brain networks," *Frontiers in Neuroscience*, vol. 4, art. 200 , 2010.

[6] V. D. Blondel, J. Guillaume, R. Lambiotte, and E. Lefebvre. "Fast unfolding of communities in large networks," *J. Stat. Mech.*, vol. 2008, p. 10008, 2008.